EVTeC 2023
6th International Electric Vehicle Technology Conference 2023

20231057

Development of Integrated On-board Converter for Wireless Power Transfer

Ryosuke Ota*[1)], Ryohei Okada**[2)], Nobukazu Hoshi***[2)]

1) *Tokyo Metropolitan University, Dept. of Electrical Engineering and Computer Science, Fac. of Systems Design, Japan*

2) *Tokyo University of Science, Dept. of Electrical Engineering, Fac. of Science and Technology, Japan*

***E-mail: r_ota@tmu.ac.jp, **E-mail: r_okada@alumni.tus.ac.jp, ***E-mail: nhoshi@rs.tus.ac.jp*

Abstract — Integrating converters for wireless power transfer (WPT) and motor drive in electric vehicles (EVs) could improve their power conversion efficiency and cost performance. This paper evaluates a proposed multiport converter that integrates WPT and motor drive systems, through both theoretical analysis and experiments. The proposed WPT system with the multiport converter is modeled to analyze its power loss in the theoretical analysis. The validity of the developed power loss models was confirmed through experiments with a prototype. Moreover, the proposed converter was compared with a conventional converter and found to be more efficient by up to 1.4 percentage points at the maximum output.

Keywords — Inductive power transfer, motor drive, electric vehicles, multiport converter, active bridge.

1. Introduction

In recent years, as a technology to extend the driving range of EVs, dynamic wireless power transfer (DWPT) is expected [1], [2]. DWPT systems need higher output power than static wireless power transfer (SWPT) systems because it is necessary to transmit enough power from the ground system to the onboard system in a short time. However, since the power loss becomes heat, to be a low-efficiency system causes an increase in the cooling system size, which oppresses the limited space in the EVs. Thus, the converters in the DWPT systems are required to be highly efficient compared to that in SWPT systems. In traction motor drive (MD) systems, the same thing, where the converter is highly efficient, is also required. Therefore, it is important to consider efficiency improvement in the onboard power electronics system in total.

Efficiency improvement methods for wireless power transfer systems are classified into several types. As one of them, there is a type making the resonant network high voltage and low current to reduce the conduction loss. For example, there is a method to connect a bidirectional DC–DC converter to the subsequent stage of the secondary-side rectifier [1], a method which uses a current doubler as the secondary side rectifier [3] and a method which uses a current-fed converter as the rectifier [4]. These methods are becoming easy year by year because of the rapid development of switching devices with wide-gap semiconductors such as SiC and GaN.

On the other hand, regarding MD systems, there is an efficiency improvement method to optimize the DC-bus voltage of the three-phase inverter based on the drive mode of the EV [5], [6]. These methods can be realized by connecting a DC–DC converter to the front stage of the inverter. This pulse amplitude modulation (PAM) can optimize a switching loss in the inverter and an iron loss in the motor [5]. In addition, the PAM-MD system can handle the high-speed rotation range of the traction motor without a high-voltage battery.

Here, it is considered that these efficiency improvement methods for WPT/MD systems are combined. However, the number of the conversion stage is also increased if the WPT system with a DC–DC converter is simply connected to the MD system with a DC–DC converter. Thus, the number of switching devices and the power losses can also be increased. To address the problem, there can be a method to connect the DC buses of the WPT/MD system to a high-voltage line made by a DC–DC converter connected to a battery [2]. However, this system is restricted from one side; thus, the control flexibility of the DC-bus voltages is reduced. Furthermore, since the voltage ratings of the WPT/MD systems need to be equal, the design flexibility is also reduced. In addition, since the DC–DC converter is a

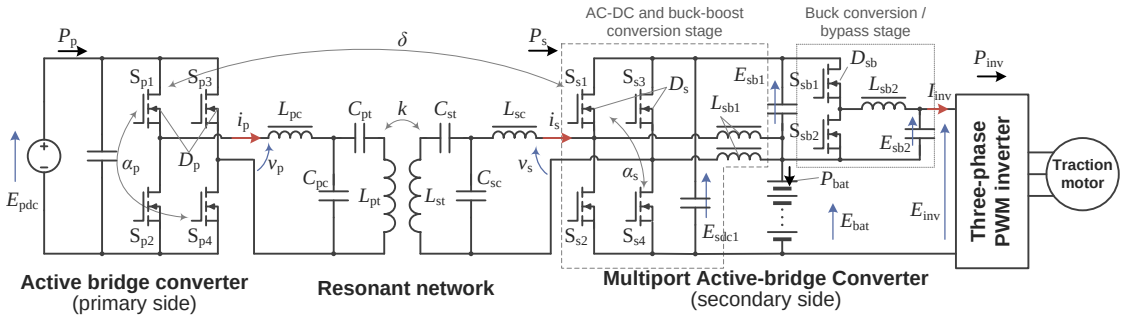

Fig. 1: Configuration of the system with the multiport active-bridge converter [7].

single-phase one, the number of phases of the converter needs to be increased when the system is applied to high-power EVs.

To address the problem, the authors have proposed a multiport active bridge (MAB) converter to integrate WPT/MD systems shown in Fig. 1 [7]. This MAB converter has two variable DC-voltage ports for the WPT/MD systems, and these DC-bus voltages can semi-independently be controlled. In addition, the number of power conversion stages is also reduced, and the efficiency can be improved. Furthermore, since the switching devices can be communized, the utilization factor of equipment of the system is high. For this, the proposed converter can handle higher power EVs compared to the conventional converters without additional DC–DC converters for interleaving.

In the previous work [7], fundamental operations of the proposed converter were confirmed using the circuit simulator *PSIM*. On the other hand, this paper develops a theoretical analysis model for the power loss in the proposed converter. In addition, the validity of the analysis model is demonstrated through experiments. Additionally, the proposed converter is compared to a conventional converter, and the effectiveness of the proposed converter is discussed.

2. Overview of Multiport Active-bridge Converter

Fig. 1 shows the system in this paper. In the primary (ground) side of this system, a typical active bridge (AB) converter is used, and the MAB converter is applied as a secondary-side (EV side) converter. Each port of the three-port MAB converter is connected to the resonant network, the battery, and the three-phase inverter for the traction motor. In addition, the MAB converter includes a buck–boost conversion stage and a buck conversion/bypass stage other than the AC–DC conversion stage. These operations are explained in the next section.

The double-sided LCC topology is adopted as the resonant network, and the transmission power P_{p} [W] is expressed as

$$P_{\mathrm{p}} = \frac{M\left|\dot{V}_{\mathrm{p}}\right|\left|\dot{V}_{\mathrm{s}}\right|}{\omega L_{\mathrm{pc}} L_{\mathrm{sc}}} \cos\phi. \tag{1}$$

Here, M [H] represents the mutual inductance between the coils L_{pt} [H] and L_{ps} [H], ω [rad/s] represents the angular frequency of the output of the AB converters, $\cos\phi$ is the power factor, and $\dot{V}_{\mathrm{p}}$ and $\dot{V}_{\mathrm{s}}$ [V] represent the phasors of the voltages v_{p} and v_{s} in both sides, respectively.

3. Operation Modes of Multiport Active-bridge Converter

Fig. 2 shows the six operation modes of the MAB converter. The MAB converter can select the operation mode according to the conditions of the DWPT charging and the driving speed of the EV. In this section, it is assumed that the state of charge (SOC) of the battery on the EV is around 50 %.

A. Low-speed Drive without DWPT Mode

In this mode, it is assumed that the EV drives at a low speed and on a normal lane without DWPT coils. In a low speed, i.e., when the revolution speed of the traction motor is low, it is not necessary to input a high voltage to the motor because its counter-electromotive force is small. For this, in this mode, the DC-bus voltage of the inverter E_{inv} [V] is set to the battery voltage E_{bat} [V] by the bypass of the switch $\mathrm{S}_{\mathrm{sb2}}$, and the conversion losses in the DC–DC converter and the inverter are reduced.

B. Medium or High-speed Drive without DWPT Mode

In this mode, since the counter-electromotive force is high, it is necessary to input a high voltage to the motor. The MAB converter works as a two-phase boost DC–DC converter

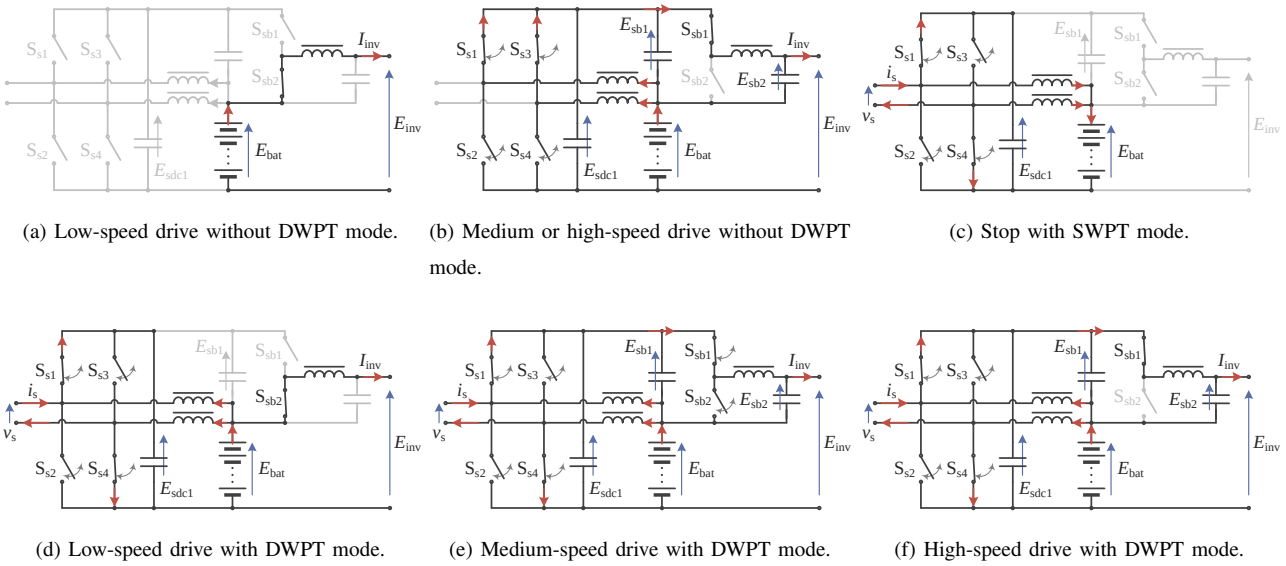

(a) Low-speed drive without DWPT mode. (b) Medium or high-speed drive without DWPT mode. (c) Stop with SWPT mode.

(d) Low-speed drive with DWPT mode. (e) Medium-speed drive with DWPT mode. (f) High-speed drive with DWPT mode.

Fig. 2: Operation modes of the multiport active-bridge converter [7].

($E_{\mathrm{sdc1}} = E_{\mathrm{inv}} \geq E_{\mathrm{bat}}$); the DC-bus voltages E_{inv} and E_{sdc1} [V] are controlled according to

$$E_{\mathrm{inv}} = E_{\mathrm{sdc1}} = \frac{E_{\mathrm{bat}}}{D_{\mathrm{s}}}. \tag{2}$$

Here, D_{s} represents the duty ratio of the upper arm switches $\mathrm{S_{s1}}$ and $\mathrm{S_{s3}}$. Since the resonant network does not need to be worked in this case, these legs are operated in phase. As a result, the conduction losses can be reduced in comparison with a single-phase converter. In other words, the MAB converter can handle higher power EVs than the single-phase boost converter.

C. Stop with SWPT Mode

In this mode, the EV stops and is charged with static WPT (SWPT). In this case, the MAB converter works as a converter, which integrates an active AC–DC and a buck conversion stages ($E_{\mathrm{sdc1}} > E_{\mathrm{bat}}$). E_{sdc1} is also expressed with (2). In addition, the AC-port in the MAB converter can be controlled according to

$$\dot{V}_{\mathrm{s\_1}} = \frac{2\sqrt{2}E_{\mathrm{sdc1}}}{\pi} \cos\frac{\alpha_{\mathrm{s}}}{2} \cos\frac{\pi\,(1-2D_{\mathrm{s}})}{2} \varepsilon^{j(\delta-(\pi-\alpha_{\mathrm{s}})/2)}, \tag{3}$$

where $\dot{V}_{\mathrm{s\_1}}$ [V] represents the fundamental-waveform component of $\dot{V}_{\mathrm{s}}$. Since the harmonic components hardly involve the transmission power in the resonant network, this paper considers only the fundamental-waveform component. In addition, α_{s} [rad] is the phase-shift angle between the legs, and δ [rad] is the phase-shift angle between the primary and secondary sides.

D. Low-speed Drive with DWPT Mode

In DWPT mode, it is assumed that the EV drives on a charging lane with DWPT systems. Since the EV drives with low speed, E_{inv} is set to E_{bat} [V] by the bypass, as well as the low-speed Drive without DWPT Mode. In addition, since the EV drives on the DWPT lane, the EV is charged according to (1), which is controlled with $\dot{V}_{\mathrm{s}}$. In this case, the power charged (discharged) to the battery P_{bat} [W] is decided according to

$$P_{\mathrm{bat}} = P_{\mathrm{p}} - P_{\mathrm{inv}}, \tag{4}$$

where P_{inv} [W] represents the output power to the inverter.

E. Medium-speed Drive with DWPT Mode

In this mode, the switches $\mathrm{S_{sb1}}$ and $\mathrm{S_{sb2}}$ work as a buck conversion stage. For this, E_{inv} is controlled in the range of $E_{\mathrm{bat}} < E_{\mathrm{inv}} < E_{\mathrm{sdc1}}$ according to the motor-drive condition and expressed as

$$E_{\mathrm{inv}} = \left\{1 + D_{\mathrm{sb}}\left(\frac{1}{D_{\mathrm{s}}} - 1\right)\right\} E_{\mathrm{bat}}, \tag{5}$$

where D_{sb} represents the duty ratio of $\mathrm{S_{sb1}}$. Furthermore, $V_{\mathrm{s\_1}}$ and P_{bat} are also expressed in (3) and (4), respectively.

F. High-speed Drive with DWPT Mode

In this mode, $\mathrm{S_{sb1}}$ works as a bypass for E_{sdc1}. In other words, that can reduce the conversion stage compared to the circuit topologies in which a general boost converter is simply connected to the subsequent AC–DC converter. In this case, E_{inv} is controlled according to (2), $V_{\mathrm{s\_1}}$ and P_{bat} are also expressed in (3) and (4), respectively.

4. Theoretical Analysis

A. Power Loss Models

In this analysis, the power losses of the MAB converter are separated into conduction losses and switching losses, and are calculated using each loss model. Here, the conduction loss P_{con} [W] in each component is derived based on the following equation.

$$P_{\mathrm{con}} = r_x I_x^2, \tag{6}$$

where r_x [Ω] represents the equivalent resistance of component X, I_x [A] represents the current in component X.

On the other hand, switching loss at turn on $P_{\mathrm{sw-on}}$ [W] and switching loss at turn off of a power device are derived based on the following equations.

$$P_{\mathrm{sw-on}} = \begin{cases} \dfrac{E_{\mathrm{sw-on\_r}} f_{\mathrm{sw}} V_{\mathrm{ds}} i_{\mathrm{d(sw-on)}}}{V_{\mathrm{ds\_r}} I_{\mathrm{d(sw-on)\_r}}} & \\ \quad + \dfrac{1}{2} C_{\mathrm{oss}} V_{\mathrm{ds}}^2 f_{\mathrm{sw}} & \text{if } i_{\mathrm{d(sw-on)}} > 0, \\ 0 & \text{if } i_{\mathrm{d(sw-on)}} < 0, \end{cases} \tag{7}$$

$$P_{\mathrm{sw-off}} = \begin{cases} \dfrac{E_{\mathrm{sw-off\_r}} f_{\mathrm{sw}} V_{\mathrm{ds}} i_{\mathrm{d(sw-off)}}}{V_{\mathrm{ds\_r}} I_{\mathrm{d(sw-off)\_r}}} & \text{if } i_{\mathrm{d(sw-off)}} > 0, \\ 0 & \text{if } i_{\mathrm{d(sw-off)}} < 0. \end{cases} \tag{8}$$

$E_{\mathrm{sw-on\_r}}$, $E_{\mathrm{sw-off\_r}}$ [J] represent one turn-on/off switching losses when the drain-source voltage V_{ds} is the reference voltage $V_{\mathrm{ds\_r}}$ [V] and the turn-on/off switching currents $i_{\mathrm{d(sw-on)}}$, $i_{\mathrm{d(sw-off)}}$ [A] are reference currents $I_{\mathrm{d(sw-on)\_r}}$, $I_{\mathrm{d(sw-off)\_r}}$ [A] in the datasheet of the power device. In addition, f_{sw} represents the switching frequency, and C_{oss} represents the output capacitance of the power device. In these power loss models, soft switching is considered, and the switching loss becomes zero when $i_{\mathrm{d(sw-on)}} < 0$ and $i_{\mathrm{d(sw-off)}} < 0$.

In this chapter, the efficiency of the MAB converter is analyzed based on the above power-loss models and the circuit parameters of the prototype shown in Table I.

B. Analysis Results

Fig. 3 shows the efficiency and power loss characteristics of the MAB converter without the DWPT operation. In addition, Fig. 4 shows the efficiency and power loss characteristics of the whole system with the DWPT operation.

In Fig. 3, the EV drives at a low speed when the output power P_{inv} is below 460 W. In this scenario, the MAB converter operates in the low-speed drive without DWPT mode, resulting in conduction losses. On the other hand, when the output power P_{inv} is above 460 W, the EV drives at a medium-to-high speed, and the MAB converter switches to the medium-to-high-speed drive without DWPT mode. In this operating mode, $\mathrm{S_{sb1}}$ functions as a bypass between the battery and the inverter, causing only conduction losses in the buck conversion/bypass stage. However, the AC–DC and buck–boost conversion stage operates in the two-phase boost operation, which causes switching losses. Consequently, Fig. 3 demonstrates a nonlinear efficiency characteristic.

In Fig. 4, when the output power P_{inv} is below 440 W, the EV drives at a low speed. In this scenario, the MAB converter operates in the low-speed drive with DWPT mode. Under these analysis conditions, the coupling coefficient k of the primary and secondary coils is assumed to be constant, and approximately 530 W is transmitted by DWPT in constant. Consequently, the losses of the primary-side converter and resonant network are also constant. In addition, the primary-side converter and the

Table I. Circuit parameters of the prototype.

Definition	value
Transmission power P_{p}	560 W (const.)
Switching frequency of $\mathrm{S_{p1}}$ – $\mathrm{S_{s4}}$ with DWPT/SWPT	85 kHz
Switching frequency of $\mathrm{S_{s1}}$ – $\mathrm{S_{s4}}$ without DWPT/SWPT	50 kHz
Switching frequency of $\mathrm{S_{b1}}$, $\mathrm{S_{b2}}$	50 kHz
Primary-side DC voltage E_{pdc}	70 V
Battery voltage E_{bat}	70 V
DC-bus voltage of the inverter E_{inv}	70 – 140 V
Transmission coils L_{pt}, L_{st}	64, 70 uH
Compensation coils L_{pc}, L_{sc}	16 , 35 uH
Coupling coefficient k	0.2
Switching devices: *ROHM* BSM080D12P2C008	
Traction motor with the three-phase inverter is simulated by a resistor	

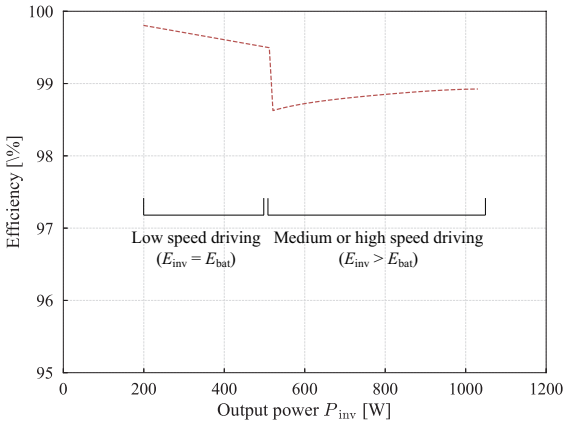

(a) Efficiency without DWPT.

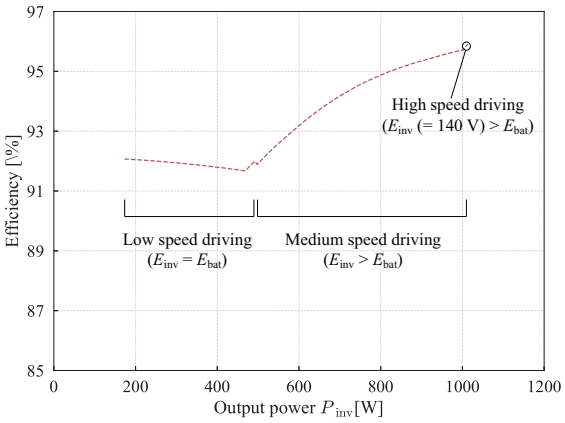

(a) Efficiency with DWPT.

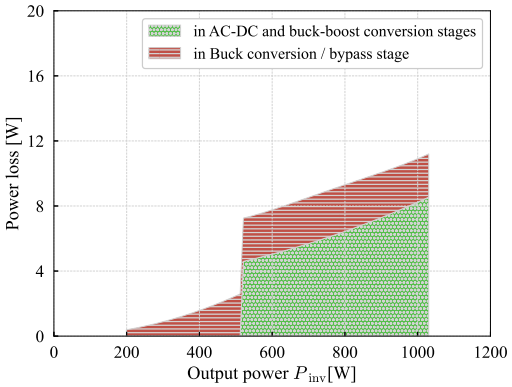

(b) Power loss without DWPT.

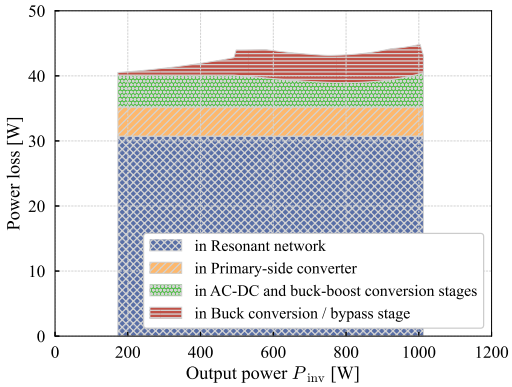

(b) Power loss with DWPT.

Fig. 3: Efficiency and power loss characteristics of the MAB converter without the DWPT operation.

Fig. 4: Efficiency and power loss characteristics of the whole system with the DWPT operation.

AC–DC and buck–boost conversion stage in the MAB converter operate with soft switching; thus, the switching loss is low, and the conduction loss is dominant.

On the other hand, when the output power P_{inv} is above 430 W, the EV drives at a medium or high speed, and the MAB converter operates in the medium-speed drive with DWPT mode. However, the MAB converter operates in the high-speed drive with DWPT mode only at the maximum output point. Since the transmission power P_{s} by DWPT is constant, the power supplied by the battery P_{bat} increases as the output power P_{inv} increases. Compared to DWPT, power supply by the boost operation from the battery is more efficient, resulting in high efficiency in the high output range.

5. Experiment

In the experiment, the validity of the analysis model is confirmed. Additionally, the proposed converter is compared to a conventional converter, and the effectiveness of the proposed converter is also confirmed with the small-scale prototype. The circuit parameters are shown in Table I. In the conventional system used in this experiment, a buck converter is connected to the subsequent stage of the secondary-side AC–DC converter for DWPT, and a boost converter is connected to the previous stage of the inverter. Except for the stop with SWPT mode, the output current to the inverter I_{inv} is regulated to 7.44 A by E_{inv} and the load resistor at $E_{\mathrm{inv}} > E_{\mathrm{bat}}$, and I_{inv} is regulated by only the load resistor at $E_{\mathrm{inv}} = E_{\mathrm{bat}}$.

Here, Fig. 5 shows the efficiency characteristics of the whole system in the experiment. In Fig. 5(a), the MAB system is

inefficient. Due to the high current capacity of the power devices used in the prototype, the switching loss is dominant in the power range of this experiment. Consequently, the total switching losses in the MAB converter are greater than in the conventional one since the MAB converter operates as a two-phase boost converter. However, at a higher output power range, the efficiency of the MAB system is expected to improve since conduction losses become dominant in the high-power range. In addition, the trend of the theoretical efficiency characteristic in Fig. 3 is generally consistent with that in Fig. 5(a).

In Fig. 5(b), it can be confirmed that the efficiency in the MAB system is efficient by 1.4 points at the maximum output point. In addition, the trend of the theoretical efficiency characteristic in Fig. 4 is also generally consistent with that in Fig. 5(b).

On the other hand, in the stop with SWPT mode, the efficiency in the MAB system is 89.7 %, and the efficiency in the conventional system is 88.2 % (though there is no graph). From the above, the validity of the power loss models of the MAB system and the partial effectiveness regarding the efficiency of the MAB converter can be confirmed.

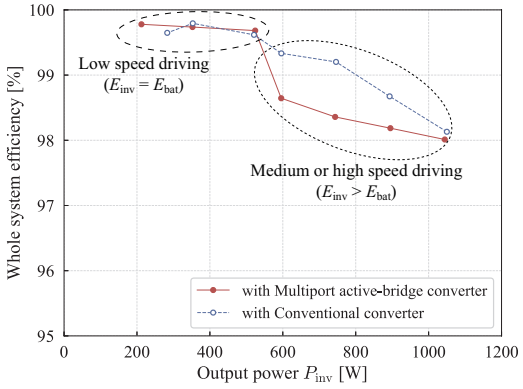

(a) Without DWPT.

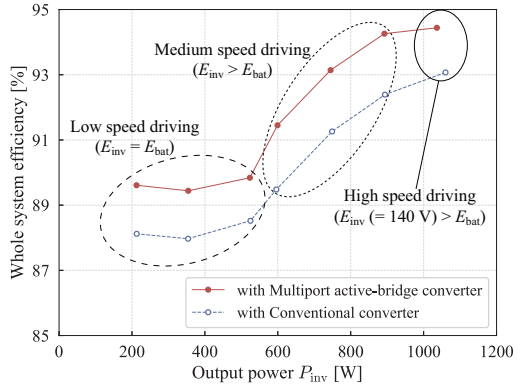

(b) With DWPT.

Fig. 5: Efficiency of the whole system in the experiment.

6. Conclusion

The overview of the MAB converter was explained. In order to analyze the MAB converter, the power loss model was shown. The trend of the efficiency characteristic by the developed power loss model is consistent with that by the experiment. In addition, it was confirmed through the experiment that the MAB system was more efficient by 1.4 percentage points than the conventional system at the maximum output point.

Acknowledgment

This work is supported by JSPS KAKENHI Grant Number JP20K14723.

References

[1] D. Kobayashi, T. Imura and Y. Hori, “Real-time Maximum Efficiency Control in Dynamic Wireless Power Transfer System,” in *IEEJ Trans. on Ind. App.*, vol. 136, no. 6, pp. 425–432, on Jun. 2016 (in Japanese).

[2] T. Takeuchi, T. Imura, D. Gunji, H. Fujimoto and Y. Hori, “Power-Flow Control Method for Wireless In-Wheel Motor with Supercapacitor,” in *IEEJ Trans. on Ind. App.*, vol. 138, no. 3, pp. 219–226, on Jun. 2018 (in Japanese).

[3] H. Z. Beh, M. Neath, J. T. Boys and G. A. Covic, “An Alternative IPT Pickup Controller for Material Handling Using a Current Doubler,” in *IEEE Trans. on Pow. Elec.*, vol. 33, no. 12, pp. 10135–10147, on Dec. 2018.

[4] G. R. Kalra, D. J. Thrimawithana, B. S. Riar, C. Huang and M. Neuburger, “A Novel Boost Active Bridge-Based Inductive Power Transfer System,” in *IEEE Trans. on Ind. Elec.*, vol. 67, no. 2, pp. 1103–1112, on Feb. 2020.

[5] A. Imakiire, K. Yamamoto and M. Hikita, “Experimental Verification on Achievement of High Efficiency Operation in Constant Power Region for Permanent Magnet Motor Driven using PWM Inverter with Voltage Booster,” in *The Japanese Journal of the Institute of Ind. App. Eng.*, vol. 4, no. 2, pp. 50–59, 2016.

[6] A. Tamura, T. Ishibashi and A. Kawamura, “EV Range Extender in a Two-Battery HEECS Chopper-Based Powertrain,” in *World Electr. Veh. J. 2019*, 10(2), 19, on Apr. 2019.

[7] R. Ota and N. Hoshi, “Basic Study of Integrated On-board Converter for Dynamic WPT EV,” in *Proc. of EVTeC 2021*, 202114320, on May 2021.